

Dysregulation of voltage-gated sodium channels by ubiquitin- ligase NEDD4-2 in neuropathic pain

Cédric J Laedermann, Matthieu Cachemaille, Guylène Kirschmann, Marie Pertin, Romain-Daniel Gosselin, Isabelle Chang, Maxime Albesa, Chris Towne, Bernard L Schneider, Stephan Kellenberger, Hugues Abriel, Isabelle Decosterd

Inventory of supplemental data

I. Supplemental Methods

II. Supplemental References

III. Supplemental Results

IV. Supplemental Figures (5)

V. Supplemental Tables (5)

Supplemental Methods

Western blots:

For *in vitro* experiments, protein extraction was performed 48 hours after transfection. HEK293 cells were lysed (50 mM Tris at pH 7.5, 150 mM NaCl, Complete Protease inhibitor cocktail tablets (Roche), 1 mM PMSF, 1% Triton) and soluble fractions were recovered in supernatants after 15 min of centrifugation at 13,000 x *g* at 4 °C. For *ex vivo* experiments, mice were sacrificed (sodium pentobarbital) and L4/L5 DRGs or sciatic nerve (from the distal trifurcation into sural, common peroneal and tibial to the proximal bifurcation into L4 and L5, neuromas were excluded) were quickly dissected. L4 and L5 DRGs or sciatic nerves from 2 mice were pooled for each sample. Lysis (100 mM Tris HCl at pH 6.8, SDS 2%, Glycerol 20% and Complete Protease inhibitor cocktail tablets) of tissues was done and soluble fractions were recovered in supernatants after 20 min centrifugation at 13,000 x *g* at 4°C. Protein concentration was measured using Bradford test-based CooAssay reagent (Uptima). Proteins were separated on acrylamide SDS-PAGE and then transferred to a nitrocellulose (HEK293) or PVDF (mouse tissue) membrane that were immunoblotted with the following antibodies: antibody to Na_v1.7 (1:500, mouse monoclonal clone N68/6, UC Davis/National Institute of Health (NIH) NeuroMab Facility, University of California), antibody to Na_v1.8 (1:200, NeuroMab), pan antibody to Na_vs (SP19, 1:500, rabbit polyclonal antibody, Sigma), antibody to NEDD4-2 (1:100, rabbit polyclonal antibody, kindly provided by O. Staub, Lausanne University), antibody to GM130 (1:500, mouse monoclonal clone 35/GM130, BD Transduction Laboratories), antibody to calreticulin (1:2000, rabbit polyclonal antibody, kindly provided by A. Abderrahmani, Lille University), antibody to BiP (1:500, rabbit monoclonal clone C50B12, Cell Signalling Technology), antibody to EEA1 (1:1000, rabbit polyclonal antibody, Abcam), antibody to LAMP1 (1:500, rabbit polyclonal antibody,

Abcam), antibody to alpha 1 subunit of the NaK/ATPase (1:5000, mouse monoclonal clone 464.6, Abcam), antibody to beta 1 subunit of the NaK/ATPase (1:1000, rabbit polyclonal antibody, kindly provided by K. Geering, Lausanne University), antibody to caveolin1 (1:200, rabbit polyclonal antibody, Santa Cruz Biotechnology) and antibody to α -tubulin (1:10,000, mouse monoclonal clone B-5-1-2) or antibody to GAPDH (1:5,000, rabbit polyclonal antibody, Abcam). For HEK293 cells we used infrared IRDyeTM (680 or 800 CW)-linked goat anti-rabbit or anti-mouse IgG (1:15,000, LI-COR Biosciences) and for mouse tissue we used secondary peroxidase-linked goat anti-rabbit or anti-mouse IgG (1:20,000, Pierce) and SuperSignal West Dura Chemiluminescent Substrate (Pierce). Protein quantification was performed using ImageJ software (US NIH).

Immunofluorescence:

Animals were transcardially perfused with saline, followed by 4% paraformaldehyde in PBS. DRGs were dissected and fixed at 4°C for 90 min and then transferred in 20% sucrose in PBS overnight. DRGs were mounted in cryoembedding fluid (Tissue-Tek, Sakura Finetek), cryosectioned at 12 μ m thickness and mounted directly onto slides.

NEDD4-2 primary antibody was used at 1:100 and Na_v1.8 (rabbit polyclonal antibody provided by S. Tate, GSK) at 1:100. Sections of DRGs were blocked for 30 min at room temperature with normal goat serum (NGS) 10% and PBS 1X-Triton X-100 0.3%. Then primary antibodies were diluted in NGS 5% and PBS 1X-Triton X100 0.1% and placed onto the sections overnight at 4°C. Slides were washed in PBS and incubated at room temperature with secondary antibodies as follows: Fluorescein (FITC)-conjugated anti-rabbit (1: 200, Jackson ImmunoResearch Laboratories) for Na_v1.8 and Cy3 anti-rabbit (1:400, Jackson ImmunoResearch Laboratories) for NEDD4-2, diluted in NGS 1% and PBS 1X-Triton X100 0.1% for 90 min. Slides were washed again in PBS and mounted with Mowiol mounting medium (Calbiochem).

Pulldown and ubiquitylation experiments:

Generation of fusion proteins: pGEX-4T1 containing GST-66 last amino acids of Nav1.7 WT and PY mutants (for pulldown experiment, Figure 3B) as well as GST-S5A (for ubiquitylation experiment, Figure 3D) were expressed in E.coli K12 cells after induction with 0.5 mM IPTG for 2 h at 30°C. Cells were resuspended in lysis buffer (20 mM Tris at pH 7.5, 250 mM NaCl, 0.5% NP40, 1 mM EDTA, 1 mM PMSF, 0.2 mg/ml DNASE I (Roche) and 0.2 mg/ml Lysozyme (Roche)) and rotated for 1 hour in the presence of GSH-Sepharose beads (Amersham Bioscience).

Pulldown: HEK293 cells were lysed for 45 minutes at 4°C with lysis buffer. Following a 15 min centrifugation at 13,000 x g at 4°C, soluble fractions were incubated with GSH-sepharose beads containing either GST (as a negative control) or the different GST fusion proteins. Pulled-down proteins were analyzed by Western Blot.

Subcellular fractionation:

HEK293 cells, DRGs and sciatic nerves were homogenized in Tris HCl 10mM, pH7.4 and 0.25M sucrose using a mortar and pestle. The lysate was charged on a sucrose gradient increasing from 15 to 50% concentration (8 fractions of 400 µl in Tris 10mM at pH 7.4) and centrifuged at 200,000 x g for 2 hours, 4°C. The whole gradient was further divided into 14 fractions of 250 µl that were analyzed by western blot.

Real time RT-PCR:

DRGs were rapidly dissected and collected in RNA-later solution (Qiagen). mRNA was extracted and purified with RNAeasy Plus Minikit (Qiagen) and quantified using RNA 6000 Nano Assay (Agilent Technologies). TaqMan mRNA Assays, specific to mRNA targets were obtained from Applied Biosystems. qRT-PCR was performed using TaqMan Fast Universal PCR Master Mix on a 7500 Fast Real-Time PCR System according to the manufacturer's

protocol. All samples were run in triplicate. Normalized signal levels for each mRNA were calculated using comparative cycle threshold method (ddCT method) relative to the mean of GAPDH or HPRT following the manufacturer's instructions.

Single cell PCR:

After whole-cell recording, single neurons were harvested and transferred to a PCR tube containing 5 μ l of Proteinase K (400 ng/ μ l) and 17 μ M of SDS. The mixture was then incubated at 50°C for 1h and at 99°C for 30 min to inactivate Proteinase K. Real-time PCR amplification and a melting curve peaking at the right temperature using beta-globin primer revealed infected cells.

Cell culture and transfection:

HEK293 cells were cultured as previously described (1). 1 μ g of Na_v1.7 cDNA or PY mutants were transfected into HEK293 cells, concomitantly with 0.8 μ g EBO-pCD-Leu2-CD8 cDNA encoding the CD8 antigen as a reporter gene and 0.8 μ g of NEDD4-2 or NEDD4-2CS. For patch clamp experiments, calcium phosphate transfection was used and for biochemistry experiments we used lipofectamine (Invitrogene). Experiments were performed 48 hours after transfection unless otherwise stated.

Neuron primary culture:

Mice (C57BL/6 mice, Charles River Lab) were sacrificed at 4-8 weeks old. L5 DRGs were harvested and digested in 5 ml of solution containing: Liberase blendzyme TM (Roche) at a concentration of 0.5U/DRG, 12 μ M EDTA in oxygenated Complete Saline Solution (CSS composition: 137 mM NaCl, 5.3 mM KCl, MgCl₂-6H₂O, 25 mM Sorbitol, 10 mM HEPES, 3 mM CaCl₂ and pH adjusted to 7.2 with NaOH) for 20 min at 37°C. Neurons were further digested with Liberase blendzyme TL in 5 ml solution (0.5U/DRG, 12 μ M EDTA in 5 ml

CSS) + Papaïn (30U/ml) for 10 min. Finally neurons were suspended in 1 ml of DRG medium Mix (89% DMEM/F-12, 10% BSA, 1% penicillin/streptomycin) supplemented with 1.5 mg of trypsin inhibitor and 1.5 mg of purified BSA. Mechanical dissociation was performed using a P1000 pipetman to gently triturate the DRG for 12 strokes. Finally, 80 µl of isolated neurons were plated on poly-D-lysine coated coverslips and incubated 12 hours before recordings to allow recovery and adhesion of neurons. Neurons were only recorded for 12 hours to prevent long-term culture phenotypic changes and neurite outgrowth that degrades space clamp.

Mouse lines:

The floxed *Nedd4L* (2) in C57BL6 background was kindly provided by O. Staub (Lausanne University). Briefly, the *Nedd4L* conditional gene targeting construct was assembled using three PCR fragments covering exons 6 through 10. One loxP site was inserted into intron 5 and the second loxP site was inserted into intron 8; this linearized targeting vector was then electroporated into ES cells to generate the homozygote floxed *Nedd4L* mouse line. This mouse line was crossed with another C57BL6 background transgenic mouse line (*Cre-SNS*) selectively expressing *Cre* recombinase in sensory ganglia using promoter elements of the $Na_v1.8$ gene (3) kindly provided by R. Kuner (Heidelberg University). A 230-kb-large bacterial artificial chromosome (BAC) containing the mouse *SCN10A* locus was identified by PCR. A cassette consisting of the *Cre* recombinase, β -actin, polyA and 500 bp homologous sequences to *SCN10a* was injected into mouse pronuclei. The two genetically modified mouse lines were backcrossed with C57BL6 mice (Charles River) for more than 8 generations. Homozygous floxed *Nedd4L* mice were crossed with *Cre* heterozygous mice in order to obtain 50% *SNS-Nedd4L*^{-/-} and 50% *Nedd4L*^{fl/fl} mice, which were then used as test animals and control littermates, respectively. Mice progeny were identified by PCR. *SNS-Cre* mice did not display any overt phenotype and were indistinguishable from wildtype when tested for thermal or mechanical sensing (3).

Viral Vector:

mNedd4L (NP_114087.2) coupled to a s-tag (provided by O. Staub, Lausanne University) was cloned into the multiple cloning site of pAAV-MCS (Stratagene) that lies downstream of the PGK promoter and β -globin intron in order to create rAAV2/6-NEDD4-2 (Figure S3A). Production and titration were performed as previously described (4). Briefly, rAAV2/6 was produced by cotransfection of the pAAV-PGK shuttle plasmid with the pDF6 packaging plasmid into the 293AAV cell line that stably expresses the E1 gene needed for activation of rep and cap promoters (5). We added proteasome inhibitor MG132 to increase viral vector production. Cell lysates were purified by high-pressure liquid chromatography on the HiTrap Heparin column (GE Healthcare Bio-Sciences AB) 48 hr later. The obtained viral suspension was concentrated with Centricon Plus-20 (Regenerated Cellulose 100,000 MWCO, Millipore) and the suspension medium replaced with PBS. The infectivity (transduction units per volume, *tu*) of the virus rAAV2/6 was determined by flow cytometry for direct eGFP fluorescence. The percentage of eGFP-positive cells was quantified 48h after infection of 293T cells with respect to uninfected control cells. The number of transduction events was calculated using the Poisson equation.

Intrathecal Injection:

Intrathecal injection were performed using Omnican U-100 insulin syringes (30Gx1/2", B.Braun). Animals backs were shaved, and mice were restrained in a towel. The needle was inserted between spinal cord L5 and L6 to deliver 3.3×10^7 *tu* (transduction units per volume) of rAAV2/6 viruses. A brief tail reflex confirmed that we attained the intrathecal space.

Electrophysiology: solutions

HEK293 cells recordings:

Whole cell patch-clamp recordings were carried-out using an internal solution containing 60 mM CsCl, 70 mM Cs Aspartate, 11 mM EGTA, 1 mM MgCl₂, 1 mM CaCl₂, 10 mM HEPES, and 5 mM Na₂-ATP, pH 7.2 with CsOH and external solution containing 130 mM NaCl, 2 mM CaCl₂, 1.2 mM MgCl₂, 5 mM CsCl, 10mM HEPES, 5 mM glucose, pH 7.4 with CsOH. For the stable cell line expressing Na_v1.7, the extracellular sodium was reduced to 50 mM and n-methyl-D-glutamine was used to substitute for sodium.

DRG neuron recordings:

The pipette solution for whole-cell measurements contained: 140 mM CsF, 10 mM NaCl, MgCl₂, 0.1 mM CaCl₂, 1.1 mM EGTA, 10 mM HEPES, pH was adjusted to 7.2 with CsOH. Extracellular solutions contained 30 mM NaCl, 110 mM TEA-Cl, 3 mM KCl, 1 mM CaCl₂, 1 mM MgCl₂, 10 mM HEPES, 10 mM Glucose, 0.1 mM CdCl, pH was adjusted to 7.3 using Tris base.

Supplemental References:

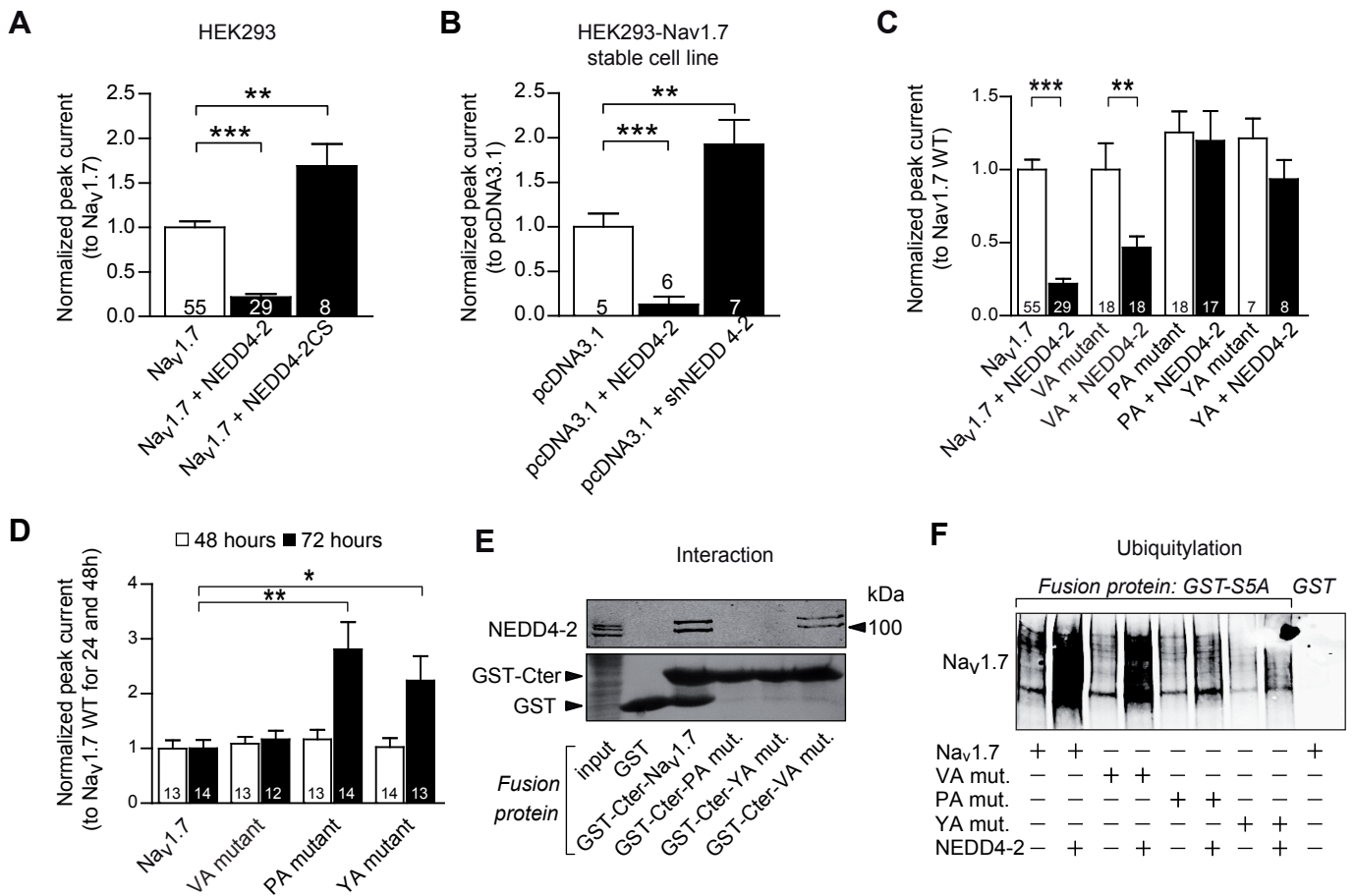
1. van Bemmelen MX, et al. Cardiac Voltage-Gated Sodium Channel Nav1.5 Is Regulated by Nedd4-2 Mediated Ubiquitination. *Circ Res.* 2004;95(3):284-291.
2. Shi PP, et al. Salt-sensitive hypertension and cardiac hypertrophy in mice deficient in the ubiquitin ligase Nedd4-2. *Am J Physiol Renal Physiol.* Aug 2008;295(2):F462-470.
3. Agarwal N, Offermanns S, Kuner R. Conditional gene deletion in primary nociceptive neurons of trigeminal ganglia and dorsal root ganglia. *Genesis.* Mar 2004;38(3):122-129.
4. Dusonchet J, Bensadoun J-C, Schneider BL, Aebischer P. Targeted overexpression of the parkin substrate Pael-R in the nigrostriatal system of adult rats to model Parkinson's disease. *Neurobiol Dis.* 2009;35(1):32-41.
5. Grimm D, Kay MA, Kleinschmidt JA. Helper virus-free, optically controllable, and two-plasmid-based production of adeno-associated virus vectors of serotypes 1 to 6. *Mol Ther.* Jun 2003;7(6):839-850.

Supplemental Results

Endogenous NEDD4-2 and PY-dependence of NEDD4-2 downregulatory effect on $\text{Na}_v1.7$ in HEK293 cells (related to Supplemental Figure 2).

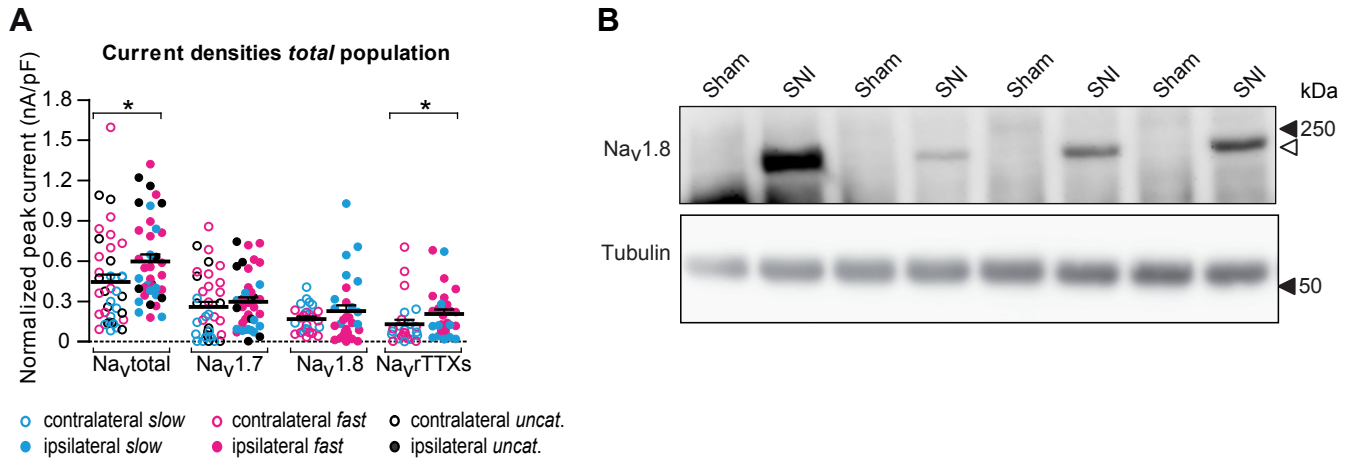
Whole-cell Na^+ current (I_{Na}) were recorded in HEK293 cells co-transfected with wild-type (WT) $\text{Na}_v1.7$ and NEDD4-2. NEDD4-2 decreased $\text{Na}_v1.7$ current density by ~80% (Supplemental Figure 2A, left, same as in Figure 2B). Conversely, co-transfection of the catalytically inactive NEDD4-2 mutant (NEDD4-2CS) increased I_{Na} density by ~70%. This effect suggests competition against endogenous NEDD4-2. Accordingly, I_{Na} density was similarly increased by NEDD4-2 silencing using shRNA in HEK293 cells stably expressing $\text{Na}_v1.7$ (Supplemental Figure 2B). Because NEDD4-2 is known to interact with the PY-motif located in the C-terminus domain of $\text{Na}_v1.7$, an alanine scan of the conserved sequence xP1P2xYxxV was performed (1). When the $\text{Na}_v1.7$ P2A (PA) and YA mutants were co-transfected with NEDD4-2, negative regulation was abolished (Supplemental Figure 2C). Conversely, a mutation within the “extended PY motif” (VA mutant) only modestly interfered with the NEDD4-2 effect (bar graph for $\text{Na}_v1.7$ WT and $\text{Na}_v1.7$ co-expressed with NEDD4-2 is the same as in Figure 2B and Supplemental Figure 2A). Because PA and YA mutants abolished the NEDD4-2 downregulatory effect, the current densities mediated by these mutants should not be subject to endogenous NEDD4-2. However PA and YA mutants current densities were not significantly increased as compared to $\text{Na}_v1.7$ WT or VA mutant. This effect is observed when at later time points after transfection. Forty eight hours after transfection, $\text{Na}_v1.7$ WT, PA, YA and VA mutants have similar current densities (Supplemental Figure 2D, white bars). When recorded 72 hours transfection, I_{Na} mediated by the PA and YA mutants were significantly increased as compared to $\text{Na}_v1.7$ WT and VA mutants, suggesting defective internalization by endogenous NEDD4-2 and accumulation of $\text{Na}_v1.7$ PY-motif mutants at the cell surface (Supplemental Figure 2D, black bars). The PY-

dependent interaction between Na_v1.7 and NEDD4-2 was further examined by pulldown experiments using GST fused to the furthest 66 C-terminal amino acid residues of Na_v1.7 (Supplemental Figure 2E is the extension of Figure 2D). WT Na_v1.7 and VA mutant GST-fusion proteins interacted with endogenous and transfected NEDD4-2 (Supplemental Figure 2E), whereas no NEDD4-2 interaction was detected with the PA and YA mutant GST-fusion proteins. Finally, whether ubiquitylation was also dependent on the PY-motif was tested (Supplemental Figure 2F is the extension of Figure 2E). Over-expression of NEDD4-2 substantially increased the GST-S5A-bound Na_v1.7 signal for WT Na_v1.7 and the VA mutant, but there was only a slight increase with the PA and YA mutants, consistent with the role of the PY-motif in this interaction (Supplemental Figure 2F).



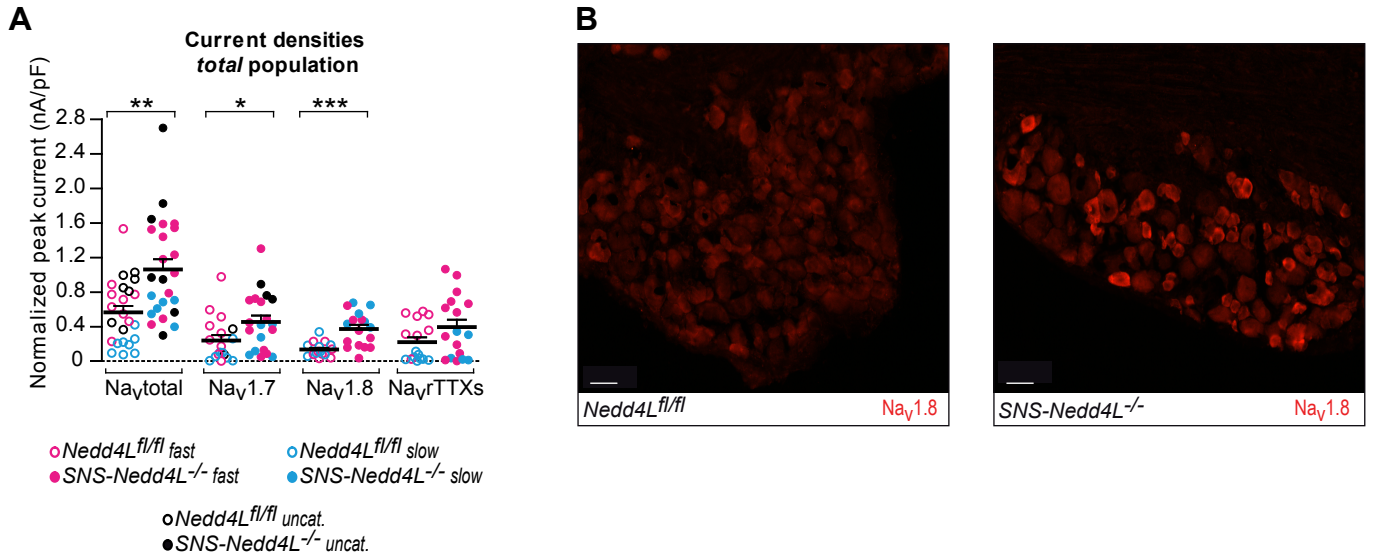
Supplemental Figure 2. NEDD4-2 downregulates Nav1.7 in a PY dependent manner.

(A) Effect of NEDD4-2 on Na_v1.7 current density in HEK293 cells. NEDD4-2 reduced WT Na_v1.7 current density ($***P < 0.001$), whereas the NEDD4-2CS inactive mutant increased I_{Na} density ($**P = 0.001$). (B) Effect of NEDD4-2 silencing on Na_v1.7 current density in Na_v1.7 HEK293 stable cell line. NEDD4-2 decreased Na_v1.7 current density ($***P < 0.001$), whereas silencing of NEDD4-2 with shRNA increased I_{Na} density ($*P = 0.025$). (C) Effect of NEDD4-2 co-transfection on WT and mutated Na_v1.7 (PY-motif mutants) current densities in HEK293 cells. NEDD4-2-related I_{Na} density downregulation was abolished in PA ($P = 0.820$) and YA ($P = 0.165$) PY-motif mutants, but not in the VA ($***P = 0.009$) mutant. See Supplementary Table 1 for values and biophysical properties. Current densities were normalized to WT Na_v1.7 (as in Figure 2B). (D) PY-motif - dependent accumulation of Na_v1.7 at the membrane. HEK293 cells were transfected with Na_v1.7 WT and PY mutants and current densities recorded 48h and 72h post-transfection. Current densities remained similar between Na_v1.7 and PY mutants (VA, PA and YA mutants) 48 h after transfection ($P > 0.05$ for each mutant). 72h after transfection, Na_v1.7 and VA mutant current densities decreased compared to 48h post-transfection (by ~58% for Na_v1.7 WT and 52% for VA mutant, not visible in the histogram due to data normalization). PA and YA mutant current densities persisted (3% increase for PA and 6% decrease for YA mutant) 72h after transfection and were significantly larger than WT Na_v1.7 currents, suggesting a defective internalization by endogenous NEDD4-2 and an accumulation of PA ($**P = 0.002$) and YA ($*P = 0.012$) mutants at the cell surface. For A to D, data are expressed as means \pm SEM. Student's *t*-test. Number of recorded cells is indicated in bars. (E) GST pulldown experiment showing Na_v1.7 PY-motif - dependent interaction with NEDD4-2. HEK293 cells were transfected with NEDD4-2 and soluble fractions were mixed with the respective GST-fusion proteins (GST-Cter-Na_v1.7 WT and GST-Cter-PY mutants). Bound NEDD4-2 was analyzed by western blot. (F) NEDD4-2-mediated ubiquitylation and PY-motif dependency. HEK293 cells were transfected with Na_v1.7 WT, VA, PA and YA mutants alone, or co-transfected with NEDD4-2 and soluble fractions were mixed with GST-S5A proteins. Bound Na_v1.7 was analyzed by western blot.



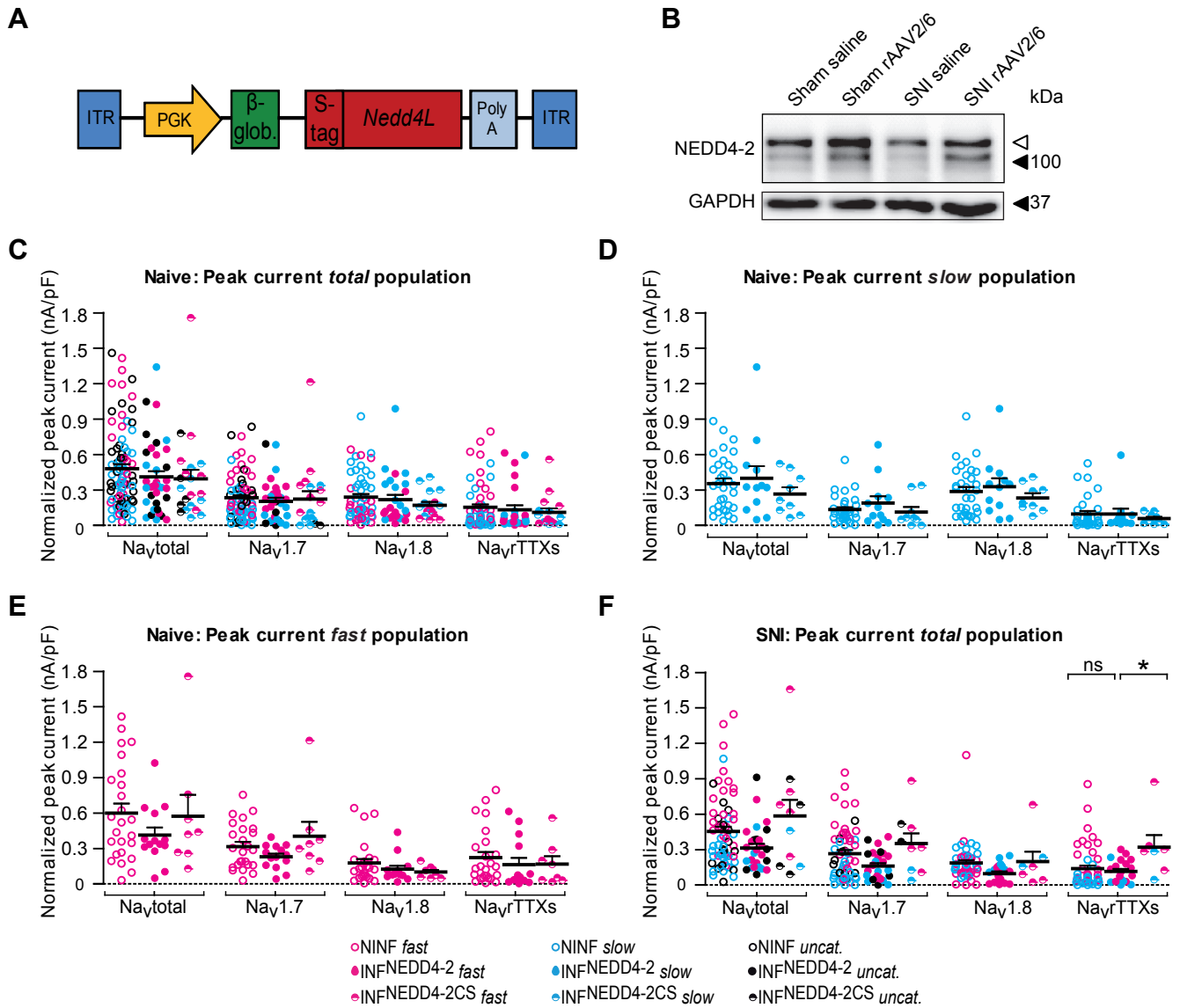
Supplemental Figure 3.

(A) Scatter dot plot representing Na_vtotal, Na_v1.7, Na_v1.8 and Na_vrTTXs current densities in contra- and ipsilateral sides recorded in L4/5 DRG neurons one week after SNI. *Slow* (in cyan, see Figure 3B also) and *fast* (in magenta, see Figure 3C also) neurons are distinguishable. In black (*uncat.* for uncategorized) are recordings that did not undergo the entire protocol. Mann Whitney test. See Supplemental Table 2 for values and biophysical properties. (B) Western blot of sciatic nerve revealed that Na_v1.8 immunoreactivity is undetectable in sham animals, but SNI induced variable signal intensity (related to Figure 3D). The open arrowheads corresponds to a distinct band of Na_v1.8, observed with lower molecular weight than 250 kDa.



Supplemental Figure 4. Immunofluorescence of Na_v1.8 from L4 DRG of *SNS-Nedd4L*^{-/-} mice and control *Nedd4L*^{fl/fl} littermates.

(A) Scattered dot plot representing Na_vtotal, Na_v1.7, Na_v1.8 and Na_vrTTXs current densities in L4/5 DRG neurons from *SNS-Nedd4L*^{-/-} and *Nedd4L*^{fl/fl} mice. *Slow* (in cyan, see Figure 4F also) and *fast* (in magenta, see Figure 4G also) neurons are distinguishable. In black (*uncat.* for uncategorized) are recordings that did not undergo the entire protocol. Mann Whitney test. See Supplemental Table 3 for values and biophysical properties. (B) Na_v1.8 immunoreactivity was almost undetectable in control mice using anti-Na_v1.8 antibody, while a distinct signal is observed in DRG of *SNS-Nedd4L*^{-/-} mice. Scale bars: 30 μm.



Supplemental Figure 5. Administration of rAAV2/6 viral vector does not modify Na_v current densities in naive animals.

(A) Schematic structure of the recombinant adeno-associated viral vector (rAAV2/6) encoding NEDD4-2 coupled to an s-tag peptide (see Methods). (B) Representative western blot of NEDD4-2 in ipsilateral L4 DRG after injection with either rAAV2/6-NEDD4-2 or saline solution. Note that endogenous NEDD4-2 has an apparent molecular weight of 120 kDa, while the virally expressed NEDD4-2 (lacking a C2 domain) migrates at 100 kDa. (C-E) Scatter dot plot representing Na_v total, Na_v 1.7, Na_v 1.8 and Na_v rTTXs current densities in non-infected cells (NINF), rAAV2/6-NEDD4-2 infected cells (INF^{Nedd4-2}) and in rAAV2/6-NEDD4-2CS (INF^{Nedd4-2CS}) in non-operated animals infected with either rAAV2/6-NEDD4-2 or rAAV2/6-NEDD4-2CS. *Slow* (in cyan, see panel D also) and *fast* (in magenta, see panel E also) neurons are distinguishable. In black (*uncat.* for uncategorized) are recordings that did not undergo the entire protocol. Non-parametric one-way analysis of variance (Kruskal-Wallis test) with Dunn *post hoc* test. For values see Supplemental Table 4. (F) same as C, but after SNI surgery for *total* population. *Slow* and *fast* neurons are shown in Figure 6E and F).

Biophysical properties of Nav1.7, Nav1.7 + NEDD4-2 and PY mutants in HEK293 cells

transfection	WT Na _v 1.7	WT + NEDD4-2	VA mutant	PA mutant	YA mutant
Activation					
V _m (mV)	-18.6 ± 0.6	-17.2 ± 0.6	-18.4 ± 0.9	-17.0 ± 0.8	-17.1 ± 0.7
slope (mV)	6.9 ± 0.2	7.7 ± 0.3	6.5 ± 0.3	7.3 ± 0.3	7.2 ± 0.5
n	26	9	14	14	9
Steady-state inactivation					
V _m (mV)	-71.6 ± 0.5	-72.4 ± 1.1	-72.9 ± 0.9	-69.9 ± 0.8	-73.0 ± 0.9
slope (mV)	8.0 ± 0.3	6.8 ± 0.5	7.7 ± 0.5	7.4 ± 0.4	9.9 ± 1.3 *
n	30	11	15	16	8
Recovery from inact.					
t _{1/2} (ms)	7.76 ± 0.38	6.48 ± 0.36	7.79 ± 0.27	7.07 ± 1.12	7.70 ± 0.63
n	23	15	15	7	6

Supplemental Table 1. Values for Na_v1.7, Na_v1.7 co-transfected with NEDD4-2 and the PY mutants in HEK cells. The V_{1/2} of steady-state activation and inactivation and their associated slope factors as well as the t_{1/2} of recovery from inactivation (see Methods) under the different conditions were not different from WT Na_v1.7, except for the slope factor of inactivation of the YA mutant. **P* < 0.05, one-way ANOVA, *post hoc* Bonferroni tests between WT Na_v1.7 and other conditions for every parameter. Data are expressed as mean ± SEM.

Biophysical properties of Na⁺ current from ipsi- and contralateral DRG neurons after SNI

		cell type	density (pA/pF)	<i>n</i>	Act. V _m (mV)	slope Act (mV)	<i>n</i>	Inact. V _m (mV)	<i>n</i>	slope Inact (mV)	RFI t _{1/2} (ms)	<i>n</i>
Na _v total	total	contralateral	444 ± 56	38	-28.1 ± 1.4	8.8 ± 0.5	35	-63.6 ± 1.7	33	10.2 ± 0.5	2.12 ± 0.17	38
		ipsilateral	598 ± 52 *	38	-27.6 ± 1.1	8.8 ± 0.3	32	-71.1 ± 2.1 **	33	8.6 ± 0.7 *	1.94 ± 0.18	35
	fast	contralateral	584 ± 111	14	-32.6 ± 1.4	7.3 ± 0.5	11	-70.5 ± 1.5	12	9.6 ± 0.8	2.69 ± 0.22	14
		ipsilateral	612 ± 72	18	-31.1 ± 1.5	7.0 ± 0.3	14	-79.2 ± 1.9 **	14	7.5 ± 0.6 *	2.07 ± 0.18 *	15
	slow	contralateral	265 ± 48	12	-22.4 ± 3.0	11.2 ± 0.5	10	-57.5 ± 2.3	10	11.6 ± 0.8	1.81 ± 0.36	12
		ipsilateral	475 ± 82 *	11	-23.63 ± 1.3	9.3 ± 0.4 **	11	-61.03 ± 3.2	11	10.1 ± 1.6	1.82 ± 0.45	11
Na _v 1.7	total	contralateral	258 ± 40	36	-31.2 ± 1.2	6.8 ± 0.4	25	-76.1 ± 1.1	20	5.8 ± 0.4	2.84 ± 0.33	18
		ipsilateral	296 ± 35	37	-28.8 ± 1.3	6.2 ± 0.2	26	-76.8 ± 1.3	21	5.0 ± 0.4	2.24 ± 0.25	20
	fast	contralateral	398 ± 62	14	-32.0 ± 1.6	6.8 ± 0.6	11	-74.8 ± 1.4	11	5.2 ± 0.6	2.76 ± 0.32	11
		ipsilateral	349 ± 51	18	-30.2 ± 1.4	5.7 ± 0.3	13	-74.0 ± 1.3	13	4.8 ± 0.3	1.90 ± 0.21 *	12
	slow	contralateral	92 ± 31	12	-26.7 ± 3.3	8.9 ± 0.9	5	-77.0 ± 3.7	4	7.2 ± 0.8	3.64 ± 0.83	5
		ipsilateral	179 ± 40 *	11	-26.4 ± 3.0	7.1 ± 0.6	7	-79.8 ± 2.8	5	5.3 ± 1.6	3.04 ± 0.63	6
Na _v 1.8	total	contralateral	168 ± 19	26	-25.6 ± 1.4	9.6 ± 0.4	21	-53.2 ± 1.3	18	6.5 ± 0.2	1.13 ± 0.07	16
		ipsilateral	227 ± 46	29	-24.5 ± 1.8	9.3 ± 0.4	19	-50.5 ± 1.1	18	5.7 ± 0.2 *	0.82 ± 0.07 **	14
	fast	contralateral	131 ± 21	14	-25.9 ± 2.5	9.1 ± 0.5	8	-52.6 ± 1.9	6	6.4 ± 0.5	1.29 ± 0.10	7
		ipsilateral	108 ± 26	18	-21.6 ± 2.8	10.0 ± 0.4	10	-51.1 ± 1.7	10	5.9 ± 0.3	0.76 ± 0.10 **	8
	slow	contralateral	209 ± 33	12	-24.0 ± 1.6	10.1 ± 0.5	10	-53.1 ± 2.0	10	6.5 ± 0.2	1.06 ± 0.10	9
		ipsilateral	421 ± 89 *	11	-27.7 ± 2.1	8.5 ± 0.6 *	9	-50.1 ± 1.7	7	5.5 ± 0.5 *	0.90 ± 0.08	6
Na _v rTTXs	total	contralateral	131 ± 34	26	-34.1 ± 2.1	8.2 ± 0.4	12	-83.1 ± 2.9	9	6.8 ± 1.0	4.81 ± 0.61	11
		ipsilateral	206 ± 33 *	29	-33.9 ± 1.3	7.6 ± 0.3	18	-80.7 ± 1.2	18	7.0 ± 0.3	3.09 ± 0.38 *	14
	fast	contralateral	165 ± 61	14	-34.2 ± 2.9	7.7 ± 0.4	6	-79.5 ± 4.8	4	8.5 ± 0.5	4.51 ± 0.32	6
		ipsilateral	249 ± 37 *	18	-34.7 ± 1.4	7.6 ± 0.3	14	-80.6 ± 1.6	13	6.8 ± 0.3 **	3.08 ± 0.41 *	13
	slow	contralateral	91 ± 23	12	-33.1 ± 4.1	9.3 ± 0.5	5	-84.6 ± 3.6	5	6.5 ± 0.8	5.17 ± 1.37	5
		ipsilateral	136 ± 61	11	-30.8 ± 3.4	7.7 ± 1.1	4	-82.6 ± 2.5	3	7.9 ± 2.0	3.3	1

Supplemental Table 2. Values for contralateral and ipsilateral DRG neurons after SNI. The capacitance (pF) was not different between the two groups (14.0 ± 0.5 pF, $n = 38$ for the contralateral side; 15.5 ± 0.6 pF, $n = 38$ for ipsilateral side, respectively. $P = 0.053$, Student's *t* test). The proportions of *fast* (14/26, 54% in contralateral and 18/29, 62% in ipsilateral) and *slow* neurons between groups were not significantly different ($\chi^2 = 0.12$, with 1 degree of freedom $P = 0.73$, chi-square test with Yates correction). SNI had a minor impact on the biophysical properties except for the 7-9 mV hyperpolarizing shift in the $V_{1/2}$ of the steady-state inactivation of Na_v total in the *total* population and *fast* subpopulation, and little modification of some slope factors. Recovery from inactivation (RFI) was accelerated for every Na_vs component in the *fast* subpopulation after SNI. Data are expressed as mean ± SEM. Student's *t*-test or Mann Whitney tests.

Biophysical properties of Na⁺ current from *Nedd4L^{fl/fl}* and *SNS-Nedd4L^{-/-}* mice DRG neurons

		cell type	density (pA/pF)	<i>n</i>	Act. V _m (mV)	slope Act (mV)	<i>n</i>	Inact. V _m (mV)	slope Inact (mV)	<i>n</i>
Na _v total	total	<i>Nedd4L^{fl/fl}</i>	565 ± 78	24	-30.8 ± 1.6	7.9 ± 0.4	23	-63.0 ± 4.4	7.8 ± 0.5	14
		<i>SNS-Nedd4L^{-/-}</i>	1062 ± 121 **	24	-38.1 ± 2.2 **	6.9 ± 0.4	21	-69.9 ± 4.0	9.9 ± 0.9 *	14
	fast	<i>Nedd4L^{fl/fl}</i>	790 ± 125	8	-35.5 ± 2.1	7.2 ± 0.4	8	-79.3 ± 2.8	7.3 ± 0.4	6
		<i>SNS-Nedd4L^{-/-}</i>	1166 ± 137	11	-38.9 ± 4.5	7.1 ± 0.8	10	-77.0 ± 3.6	9.0 ± 1.1	7
	slow	<i>Nedd4L^{fl/fl}</i>	195 ± 43	8	-23.7 ± 1.5	9.9 ± 0.4	6	-51.0 ± 2.7	8.2 ± 0.9	6
		<i>SNS-Nedd4L^{-/-}</i>	617 ± 58 **	6	-34.2 ± 2.5 **	7.1 ± 0.6 **	4	-54.0 ± 3.9	10.5 ± 1.4	4
Na _v 1.7	total	<i>Nedd4L^{fl/fl}</i>	241 ± 63	18	-31.9 ± 2.4	6.1 ± 0.4	15	-78.7 ± 1.5	7.4 ± 0.9	6
		<i>SNS-Nedd4L^{-/-}</i>	455 ± 77 *	20	-36.2 ± 2.7	5.8 ± 0.4	14	-80.2 ± 2.0	5.6 ± 0.6	7
	fast	<i>Nedd4L^{fl/fl}</i>	415 ± 108	8	-36.7 ± 2.6	5.5 ± 0.5	7	-77.2 ± 2.9	8.75 ± 3.7	2
		<i>SNS-Nedd4L^{-/-}</i>	487 ± 116	11	-36.1 ± 3.9	5.9 ± 0.6	8	-77.7	3.5	1
	slow	<i>Nedd4L^{fl/fl}</i>	70 ± 33	8	-25.4 ± 4.1	7.3 ± 0.6	6	-79.5 ± 2.1	6.8 ± 0.5	4
		<i>SNS-Nedd4L^{-/-}</i>	487 ± 116 *	6	-27.9 ± 2.0	6.9 ± 0.5	3	-79.2 ± 2.4	5.7 ± 0.6	5
Na _v 1.8	total	<i>Nedd4L^{fl/fl}</i>	132 ± 20	17	-28.4 ± 1.5	9.8 ± 0.7	17	-56.6 ± 1.7	6.7 ± 0.5	14
		<i>SNS-Nedd4L^{-/-}</i>	371 ± 50 ***	17	-32.9 ± 2.9	11.4 ± 1.3	12	-54.6 ± 1.9	5.4 ± 0.3 *	12
	fast	<i>Nedd4L^{fl/fl}</i>	117 ± 29	8	-28.3 ± 1.8	11.2 ± 0.9	8	-54.7 ± 2.7	7.1 ± 0.9	7
		<i>SNS-Nedd4L^{-/-}</i>	286 ± 58 *	11	-34.7 ± 5.3	12.5 ± 1.5	7	-55.4 ± 3.2	5.8 ± 0.4	7
	slow	<i>Nedd4L^{fl/fl}</i>	152 ± 34	8	-27.4 ± 3.3	8.9 ± 1.1	7	-58.6 ± 2.5	6.4 ± 0.7	6
		<i>SNS-Nedd4L^{-/-}</i>	527 ± 53 ***	6	-32.0 ± 3.4	8.3 ± 0.6	5	-53.5 ± 1.8	4.8 ± 0.3	5
Na _v rTTXs	total	<i>Nedd4L^{fl/fl}</i>	220 ± 59	16	-39.7 ± 1.7	6.9 ± 0.5	10	-85.0 ± 2.0	8.2 ± 1.0	6
		<i>SNS-Nedd4L^{-/-}</i>	394 ± 90	17	-43.6 ± 2.8	7.1 ± 0.4	9	-88.1 ± 1.6	7.4 ± 0.7	7
	fast	<i>Nedd4L^{fl/fl}</i>	399 ± 72	8	-40.9 ± 2.1	7.3 ± 0.6	6	-84.1 ± 2.2	7.4 ± 0.5	5
		<i>SNS-Nedd4L^{-/-}</i>	544 ± 112	11	-46.6 ± 2.5	7.2 ± 0.4	7	-88.4 ± 1.6	7.4 ± 0.8	5
	slow	<i>Nedd4L^{fl/fl}</i>	42 ± 14	8	-33.4 ± 4.4	7.2 ± 0.3	2	-89.3	12.1	1
		<i>SNS-Nedd4L^{-/-}</i>	119 ± 71	6	-33.2 ± 1.2	6.6 ± 1.5	2	-87.5 ± 3.6	7.6 ± 2.7	2

Supplemental Table 3. Values for *SNS-Nedd4L^{-/-}* and *Nedd4L^{fl/fl}* DRG neurons. The capacitance (pF) was not different between the two groups (13.8 ± 0.8 pF, $n = 24$ and 13.5 ± 0.8 pF, $n = 24$, $P = 0.84$, Student's *t* test). *Fast* neurons correspond to 50% of *Nedd4L^{fl/fl}* (8/16) and 65% of *SNS-Nedd4L^{-/-}* (11/17). The proportion of *fast* and *slow* neurons between genotypes was not different ($\chi^2 = 0.25$, with 1 degree of freedom $P = 0.62$, chi-square test with Yates correction). The two mice lines had the same biophysical properties except for the 10 mV hyperpolarizing shift in the $V_{1/2}$ of activation of Na_vtotal in the *total* population and *slow* subpopulation, and little modification of some slope factors. Data are expressed as mean ± SEM. Student's *t*-test or Mann Whitney tests.

Biophysical properties of Na⁺ current of DRG neurons from naive mice infected with either rAAV2/6-NEDD4-2 or rAAV2/6-NEDD4-2CS

		cell type	density (pA/pF)	n	Act. Vm (mV)	slope Act. (mV)	n	Inact. Vm (mV)	slope Inact. (mV)	n	RFI t _{1/2} (ms)	n
Na _v total	total	NINF	457 ± 41	85	-26.9 ± 0.9	8.3 ± 0.2	71	-62.9 ± 1.7	10.3 ± 0.4	51	2.35 ± 0.20	41
		INF ^{NEDD4-2}	410 ± 50	37	-24.3 ± 1.3	9.0 ± 0.5	33	-57.3 ± 2.5	9.7 ± 0.6	24	1.86 ± 0.21	22
		INF ^{NEDD4-2CS}	394 ± 80	22	-24.6 ± 1.9	8.6 ± 0.5	20	-55.2 ± 5.2	7.4 ± 0.7 ***	12	1.46 ± 0.26	13
	fast	NINF	600 ± 83	25	-30.4 ± 1.5	7.4 ± 0.3	20	-69.7 ± 1.9	10.9 ± 0.6	14	2.94 ± 0.43	12
		INF ^{NEDD4-2}	413 ± 69	14	-27.1 ± 2.0	8.1 ± 0.6	12	-69.2 ± 2.5	9.4 ± 0.7	8	2.51 ± 0.46	7
		INF ^{NEDD4-2CS}	573 ± 195	8	-31.7 ± 2.8	7.3 ± 0.7	7	-75.8 ± 2.6	6.5 ± 0.2	4	2.41 ± 0.34	4
	slow	NINF	356 ± 42	32	-22.7 ± 0.9	9.1 ± 0.4	29	-53.1 ± 2.1	11.0 ± 0.8	19	1.66 ± 0.25	13
		INF ^{NEDD4-2}	399 ± 107	12	-24.2 ± 2.3	9.1 ± 0.8	12	50.5 ± 4.0	9.0 ± 1.6	7	1.56 ± 0.36	7
		INF ^{NEDD4-2CS}	265 ± 61	9	-19.62 ± 2.0	9.6 ± 0.7	9	-44.9 ± 4.1	8.4 ± 1.7	4	1.0 ± 0.22	4
Na _v 1.7	total	NINF	235 ± 22	75	-27.5 ± 1.0	7.5 ± 0.3	49	-75.0 ± 1.0	7.2 ± 0.9	23	3.08 ± 0.28	19
		INF ^{NEDD4-2}	205 ± 31	32	-28.2 ± 1.8	7.5 ± 0.7	18	-74.4 ± 1.4	7.6 ± 0.7	9	2.46 ± 0.29	9
		INF ^{NEDD4-2CS}	224 ± 67	19	-28.2 ± 2.3	7.7 ± 0.8	12	-72.6 ± 1.6	5.3 ± 0.8	7	2.27 ± 0.20	6
	fast	NINF	317 ± 40	25	-29.1 ± 1.5	6.9 ± 0.4	21	-73.2 ± 1.8	6.7 ± 0.9	10	3.12 ± 0.45	9
		INF ^{NEDD4-2}	230 ± 28	14	-28.1 ± 2.5	7.1 ± 0.7	10	-74.3 ± 2.5	7.6 ± 0.8	5	2.37 ± 0.55	5
		INF ^{NEDD4-2CS}	404 ± 131	8	-31.6 ± 3.1	6.5 ± 0.8	7	-72.7 ± 3.1	4.3 ± 0.9	4	2.21 ± 0.32	4
	slow	NINF	137 ± 21	32	-23.8 ± 1.5	8.4 ± 0.5	20	-75.2 ± 1.6	7.0 ± 1.9	8	3.02 ± 0.48	7
		INF ^{NEDD4-2}	188 ± 61	12	-29.0 ± 3.9	7.0 ± 1.5	6	-73.8 ± 2.2	7.8 ± 2.4	3	2.72 ± 0.23	3
		INF ^{NEDD4-2CS}	112 ± 46	9	-23.5 ± 2.6	9.3 ± 1.5	5	-72.6 ± 0.9	6.7 ± 0.9	3	2.3	1
Na _v 1.8	total	NINF	239 ± 27	57	-25.6 ± 1.0	9.3 ± 0.3	44	-47.6 ± 0.7	5.9 ± 0.3	34	0.76 ± 0.04	28
		INF ^{NEDD4-2}	218 ± 43	26	-25.6 ± 1.5	8.6 ± 0.6	20	-48.5 ± 1.0	6.0 ± 0.6	17	0.85 ± 0.07	16
		INF ^{NEDD4-2CS}	171 ± 29	17	-20.4 ± 1.4	9.8 ± 0.5	10	-48.5 ± 0.8	6.2 ± 0.3	10	0.71 ± 0.03	10
	fast	NINF	177 ± 36	25	-27.5 ± 1.5	9.5 ± 0.6	16	-49.3 ± 1.1	6.3 ± 0.4	13	0.82 ± 0.06	12
		INF ^{NEDD4-2}	124 ± 31	14	-22.9 ± 1.2	9.5 ± 0.7	10	-49.6 ± 1.6	6.4 ± 1.2	9	0.79 ± 0.08	8
		INF ^{NEDD4-2CS}	101 ± 20	8	-19.2 ± 1.6 **	10.6 ± 0.5	6	-50.1 ± 0.8	6.6 ± 0.2	6	0.75 ± 0.03	6
	slow	NINF	285 ± 38	32	-25.1 ± 1.4	9.0 ± 0.5	26	-46.6 ± 0.8	5.7 ± 0.3	21	0.82 ± 0.06	16
		INF ^{NEDD4-2}	327 ± 76	12	-28.2 ± 2.6	7.8 ± 0.9	10	-47.3 ± 1.1	5.6 ± 0.4	8	0.79 ± 0.08	7
		INF ^{NEDD4-2CS}	234 ± 41	9	-22.2 ± 3.0	8.58 ± 0.8	4	-46.0 ± 0.7	5.7 ± 0.6	4	0.75 ± 0.03	4
Na _v TTXs	total	NINF	153 ± 26	57	-32.7 ± 1.5	8.3 ± 0.5	27	-80.1 ± 1.0	6.9 ± 0.6	16	3.37 ± 0.35	16
		INF ^{NEDD4-2}	132 ± 38	26	-29.9 ± 2.3	8.4 ± 0.7	11	-78.6 ± 2.0	9.5 ± 1.3	8	3.41 ± 1.06	6
		INF ^{NEDD4-2CS}	110 ± 35	17	-31.3 ± 3.0	9.8 ± 1.0	8	-83.6 ± 1.1	6.6 ± 0.7	5	3.66 ± 0.72	4
	fast	NINF	223 ± 48	25	-34.9 ± 2.0	7.9 ± 0.6	14	-80.5 ± 1.0	7.7 ± 0.6	9	3.64 ± 0.49	9
		INF ^{NEDD4-2}	163 ± 59	14	-31.0 ± 1.0	8.1 ± 0.6	7	-80.1 ± 0.7	8.9 ± 1.8	5	3.93 ± 1.65	4
		INF ^{NEDD4-2CS}	169 ± 70	8	-31.5 ± 3.4	9.7 ± 1.1	7	-82.9 ± 1.0	6.9 ± 0.7	4	3.07 ± 0.35	3
	slow	NINF	100 ± 24	32	-30.3 ± 2.2	8.7 ± 0.9	13	-79.6 ± 2.2	5.9 ± 0.9	7	3.02 ± 0.54	7
		INF ^{NEDD4-2}	96 ± 48	12	-28.1 ± 7.3	8.9 ± 1.8	4	-76.0 ± 6.2	10.4 ± 2.6	3	2.37 ± 0.70	2
		INF ^{NEDD4-2CS}	57 ± 16	9	-29.4	10.4	1	-86.4	5.1	1	5.44	1

Supplemental Table 4. Values for cells transduced with rAAV2/6-NEDD4-2 (INF^{NEDD4-2}) and control cells either transduced with rAAV2/6-NEDD4-2CS (INF^{NEDD4-2CS}) or not transduced (NINF) in naive animals. The capacitance (pF) was significantly higher in cells infected with rAAV2/6-NEDD4-2 (15.4 ± 0.4 pF with $n = 85$ for NINF, 17.4 ± 0.7 with $n = 37$ for INF^{NEDD4-2} and 15.5 ± 0.7 pF with $n = 22$ for INF^{NEDD4-2CS}, $P < 0.05$ between NINF and INF^{NEDD4-2} cells, Kruskal-Wallis and *post hoc* Dunn tests). NINF cells recorded from each group of vector-injected animals exhibited no differences in the current densities of any of the components and were thus pooled into one group. Data are expressed as mean ± SEM. One-way ANOVA (*post hoc* Bonferroni tests) or Kruskal-Wallis test (Dunn *post hoc* test).

Biophysical properties of Na⁺ current of DRG neurons from mice infected with either rAAV2/6-NEDD4-2 or rAAV2/6-NEDD4-2CS after SNI

		cell type	density (pA/pF)	n	Act. Vm (mV)	slope Act. (mV)	n	Inact. Vm (mV)	slope Inact. (mV)	n	RFI t _{1/2} (ms)	n
Na _v total	total	NINF	455 ± 41	63	-26.4 ± 1.0	8.5 ± 0.3	55	-61.0 ± 2.0	8.8 ± 0.4	46	1.99 ± 0.13	45
		INF ^{NEDD4-2}	313 ± 37	28	-26.0 ± 1.8	8.4 ± 0.4	25	-62.5 ± 3.0	7.9 ± 0.5	21	2.10 ± 0.18	19
		INF ^{NEDD4-2CS}	585 ± 143	11	-31.6 ± 2.1	7.6 ± 0.7	8	-70.0 ± 3.0	8.8 ± 1.5	5	1.98 ± 0.26	5
	fast	NINF	650 ± 69	25	-30.2 ± 1.3	7.3 ± 0.3	24	-69.5 ± 1.3	9.58 ± 0.5	20	2.33 ± 0.12	20
		INF ^{NEDD4-2}	334 ± 48 **	13	-27.3 ± 1.2	8.1 ± 0.5	11	-70.1 ± 0.9	6.6 ± 0.5 **	9	2.26 ± 0.17	9
		INF ^{NEDD4-2CS}	798 ± 261 *	5	-33.6 ± 1.9	6.2 ± 0.5	4	-72.1 ± 3.7	6.8 ± 1.0	3	1.91 ± 0.41	3
	slow	NINF	287 ± 46	22	-19.5 ± 1.4	10.2 ± 0.5	18	-46.9 ± 2.3	8.4 ± 0.6	15	1.30 ± 0.18	14
		INF ^{NEDD4-2}	222 ± 52	7	-19.7 ± 3.8	9.2 ± 1.3	7	-49.7 ± 5.4	7.9 ± 1.0	5	1.82 ± 0.39	4
		INF ^{NEDD4-2CS}	309 ± 213	2	-25.5 ± 8.0	9.5 ± 1.4	2					
Na _v 1.7	total	NINF	266 ± 30	57	-26.8 ± 1.1	7.4 ± 0.3	40	-73.6 ± 1.0	6.8 ± 0.9	22	2.42 ± 0.16	25
		INF ^{NEDD4-2}	160 ± 24	26	-25.2 ± 1.3	7.4 ± 0.4	15	-70.8 ± 2.7	7.0 ± 1.5	5	1.68 ± 0.18 *	9
		INF ^{NEDD4-2CS}	351 ± 92	9	-30.2 ± 2.3	7.0 ± 0.7	6	-71.8 ± 2.3	4.1 ± 0.7	2	1.68 ± 0.45	3
	fast	NINF	412 ± 47	25	-29.8 ± 1.1	6.5 ± 0.3	23	-73.7 ± 1.0	6.1 ± 0.4	15	2.31 ± 0.16	15
		INF ^{NEDD4-2}	193 ± 34 **	13	-26.3 ± 1.3	7.4 ± 0.4	10	-69.6 ± 3.1	7.3 ± 1.9	4	1.53 ± 0.22 *	6
		INF ^{NEDD4-2CS}	421 ± 145	5	-37.3 ± 2.6	6.1 ± 0.4	4	-71.8 ± 2.3	4.1 ± 0.7	2	1.68 ± 0.45	3
	slow	NINF	120 ± 25	22	-22.9 ± 1.7	8.2 ± 0.5	11	-74.9 ± 3.9	9.9 ± 4.1	5	3.14 ± 0.22	7
		INF ^{NEDD4-2}	85 ± 28	7	-20.49 ± 3.5	7.3 ± 1.3	3					
		INF ^{NEDD4-2CS}	83 ± 63	2	-22.5	9.4	1					
Na _v 1.8	total	NINF	187 ± 25	46	-25.0 ± 1.1	9.5 ± 0.3	33	-48.4 ± 0.7	5.9 ± 0.2	31	0.86 ± 0.05	29
		INF ^{NEDD4-2}	98 ± 18 *	20	-25.0 ± 1.8	9.6 ± 0.8	10	-50.7 ± 1.1	5.7 ± 0.3	10	0.85 ± 0.06	9
		INF ^{NEDD4-2CS}	199 ± 92	7	-28.9 ± 1.9	9.5 ± 0.7	5	-51.1 ± 1.4	5.6 ± 0.4	4	0.71 ± 0.06	5
	fast	NINF	140 ± 18	25	-26.0 ± 1.5	9.9 ± 0.4	17	-49.8 ± 0.9	6.4 ± 0.5	15	0.90 ± 0.06	15
		INF ^{NEDD4-2}	59 ± 16 *	13	-23.4 ± 2.5	11.2 ± 0.6	4	-52.9 ± 0.6	6.2 ± 0.4	5	0.86 ± 0.08	5
		INF ^{NEDD4-2CS}	199 ± 137	5	-29.4 ± 1.8	9.7 ± 1.4	3	-52.3 ± 1.1	5.9 ± 0.2	2	0.71 ± 0.10	3
	slow	NINF	239 ± 46	22	-23.6 ± 1.7	9.0 ± 0.6	14	-47.1 ± 1.1	5.4 ± 0.2	16	0.82 ± 0.07	16
		INF ^{NEDD4-2}	170 ± 22	7	-26.1 ± 2.8	8.5 ± 1.1	6	-48.5 ± 1.7	5.1 ± 0.2	5	0.83 ± 0.12	4
		INF ^{NEDD4-2CS}	197 ± 53	2	-21.1 ± 6.6	9.3 ± 0.2	2	-49.9 ± 3.4	5.3 ± 0.8	2	0.72 ± 0.17	2
Na _v rTTXs	total	NINF	142 ± 27	46	-31.5 ± 1.5	8.7 ± 0.5	21	-80.0 ± 1.5	7.5 ± 0.5	21	3.80 ± 0.31	19
		INF ^{NEDD4-2}	116 ± 22	20	-32.3 ± 1.3	8.5 ± 0.5	13	-79.9 ± 1.6	7.2 ± 0.7	6	3.56 ± 0.49	8
		INF ^{NEDD4-2CS}	322 ± 108 *	7	-39.3 ± 1.4 *	6.7 ± 0.9	6	-81.6 ± 2.7	6.4 ± 0.3	3	2.38 ± 0.41	2
	fast	NINF	220 ± 44	25	-32.6 ± 1.8	8.6 ± 0.6	16	-79.2 ± 2.0	8.1 ± 0.6	15	3.80 ± 0.42	13
		INF ^{NEDD4-2}	149 ± 25	13	-32.2 ± 1.6	8.9 ± 0.6	10	-79.1 ± 1.6	6.7 ± 0.6	5	3.56 ± 0.49	8
		INF ^{NEDD4-2CS}	384 ± 143	5	-39.6 ± 1.4	6.2 ± 1.0	4	-81.6 ± 2.7	6.4 ± 0.3	3	2.38 ± 0.41	2
	slow	NINF	50 ± 12	22	-26.5 ± 2.6	9.1 ± 1.1	4	-81.9 ± 1.9	6.4 ± 0.8	6	3.81 ± 0.44	6
		INF ^{NEDD4-2}	54 ± 33	7	-33.0 ± 2.6	7.3 ± 0.5	3	-84.0	9.8	1		
		INF ^{NEDD4-2CS}	166 ± 169	2	-38.9 ± 5.6	7.9 ± 2.3	2					

Supplemental Table 5. Values for cells transduced with rAAV2/6-Nedd4-2 (INF^{NEDD4-2}) and control cells either transduced with rAAV2/6-Nedd4-2CS (INF^{NEDD4-2CS}) or not transduced (NINF) after SNI. The capacitance (pF) was not significantly different between groups (15.9 ± 0.5 pF with n = 63 for NINF, 16.4 ± 0.8 with n = 28 for INF^{NEDD4-2} and 15.3 ± 1.0 pF with n = 11 for INF^{NEDD4-2CS}, P = 0.832. NINF cells recorded from animals injected with rAAV2/6-NEDD4-2 or rAAV2/6-NEDD4-2CS exhibited no difference in the peak I_{Na} densities and were thus pooled in one group. Data are expressed as mean ± SEM. One-way ANOVA (post hoc Bonferroni tests) or Kruskal-Wallis test (Dunn post hoc test).